

Highly Efficient and Selective Photocatalytic Oxidation of Sulfide by a Chromophore–Catalyst Dyad of Ruthenium-Based Complexes

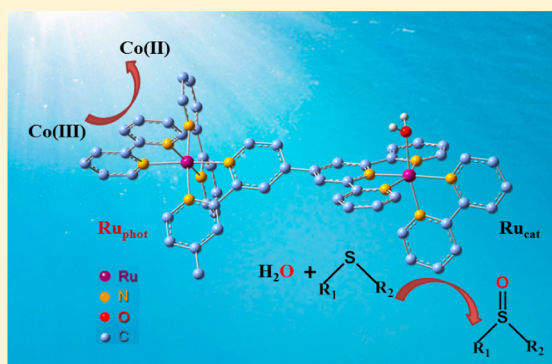
Ting-Ting Li,[†] Fu-Min Li,[‡] Wei-Liang Zhao,[‡] Yong-Hua Tian,[‡] Yong Chen,[†] Rong Cai,[†] and Wen-Fu Fu^{*,†,‡}

[†]Key Laboratory of Photochemical Conversion and Optoelectronic Materials and HKU-CAS Joint Laboratory on New Materials, Technical Institute of Physics and Chemistry and University of Chinese Academy of Sciences, CAS, Beijing 100190, People's Republic of China

[‡]College of Chemistry and Engineering, Yunnan Normal University, Kunming 650092, People's Republic of China

Supporting Information

ABSTRACT: Electronic coupling across a bridging ligand between a chromophore and a catalyst center has an important influence on biological and synthetic photocatalytic processes. Structural and associated electronic modifications of ligands may improve the efficiency of photocatalytic transformations of organic substrates. Two ruthenium-based supramolecular assemblies based on a chromophore–catalyst dyad containing a Ru–aqua complex and its chloro form as the catalytic components were synthesized and structurally characterized, and their spectroscopic and electrochemical properties were investigated. Under visible light irradiation and in the presence of $[\text{Co}(\text{NH}_3)_5\text{Cl}]\text{Cl}_2$ as a sacrificial electron acceptor, both complexes exhibited good photocatalytic activity toward oxidation of sulfide into the corresponding sulfoxide with high efficiency and >99% product selectivity in neutral aqueous solution. The Ru–aqua complex assembly was more efficient than the chloro complex. Isotopic labeling experiments using ^{18}O -labeled water demonstrated the oxygen atom transfer from the water to the organic substrate, likely through the formation of an active intermediate, $\text{Ru}(\text{IV})=\text{O}$.



INTRODUCTION

Development of photocatalytic methods for organic transformations is an important aspect of renewable energy technologies. The enormous potential of solar energy as a clean and economical energy source motivates the development of new methods to convert solar to chemical energy.¹ In oxygenic photosynthesis, oxidation of water into molecular oxygen is activated by a high-valent manganese–oxo cluster in the dark at photosystem II.² This reaction has inspired numerous efforts toward developing photocatalytic conversions of organic substrates.³ The use of high-valent metal–oxo complexes in organic transformations is essential because of their irreplaceable roles as reactive intermediates in biological and synthetic redox reactions.⁴ Since the pioneering work reported by Gray and his colleagues,⁵ many $\text{Fe}(\text{IV})$ –, $\text{Mn}(\text{IV})$ –, and $\text{Ru}(\text{IV})$ –oxo complexes have been found to take part in a stepwise photoinduced proton-coupled electron transfer (PCET) through the interaction of their initial low-valent metal–aqua complexes and oxidized photosensitizers such as $[\text{Ru}^{\text{III}}(\text{bpy})_3]^{3+}$ or $[\text{Ru}^{\text{III}}(\text{tpy})_3]^{3+}$ (bpy = 2,2'-bipyridine; tpy = 2,2':6'2''-terpyridine).⁶ Recently, light-driven sulfide oxygenation reactions using chromophore–catalyst dyad photocatalysts have attracted considerable attention from many research groups for their fundamental interest and potential applications in the pharmaceutical and petroleum industries.⁷

Previous studies have shown that the oxygenation of organic sulfides can be carried out using either H_2O_2 or $t\text{BuOOH}$.⁸ However, these compounds have disadvantages in terms of their thermal instability and poor selectivity, which limit their practical application in industry. Photocatalytic sulfide oxygenation by high-valent metal–oxo complexes in aqueous systems remains relatively unexplored because the reactions involve a two-electron and two-proton transfer process.⁹ In this context, photocatalytic sulfide oxygenation systems have the following requirements: (1) the chromophore should efficiently harvest light in the visible spectrum, (2) the system should feature rapid and effective excited-state electron transfer with minimal recombination between the catalyst and chromophore, and (3) water should be the source of the oxygen atom.

Combining a chromophore with a catalytic fragment to form a supramolecular photocatalyst could meet these requirements. This would accelerate the successive electron transfer steps in the correct direction, diminish electron recombination, and enable more efficient performance of a dyad compared with a bimolecular system. Additionally, this may simplify the study of the different processes for mononuclear homologues.¹⁰

Received: August 28, 2014

Our group is interested in the design of a supramolecule that combines a chromophore and a catalytic fragment within the same entity to improve the photocatalytic reaction efficiency compared with that of bimolecular systems. One $[\text{Ru}^{\text{II}}(\text{bpy})_3]^{2+}$ or $[\text{Ru}^{\text{II}}(\text{tpy})_3]^{2+}$ moiety was chosen to act as the light-harvesting antenna, and another unit behaved as a catalyst connected by a bridging ligand. Our investigations of the photophysical properties and catalytic activity as well as other groups' work revealed that the bridging ligands play a crucial role in catalytic performance and impact the lifetime of the excited states, the directionality of the electron transfer, and the redox potentials of both units.¹¹ We have also found that the photocatalytic efficiency of the two moieties in a supramolecule linked through a carbon–carbon single bond is superior to that of a double bond connection in either photocatalytic CO_2 reduction or light-driven oxygenation of alcohols.^{11a–c} We have now begun to focus on designing supramolecular catalysts to improve the performance of photocatalytic sulfide oxygenation. An assembly with the well-studied photosensitizer $[\text{Ru}(\text{bpy})_3]^{2+}$ and the versatile catalyst $[\text{Ru}(\text{bpy})(\text{tpy})(\text{X})]^{n+}$ ($\text{X} = \text{Cl}, \text{H}_2\text{O}$) has been used in a variety of chemical transformations, including water oxidation,¹² organic substrate oxygenation,^{9,10e,11a,b} and reduction of CO_2 .¹³ We assumed the induction of $[\text{Ru}(\text{bpy})_3]^{2+}$ having a long excited-state lifetime and a single bond linkage may improve the photocatalytic efficiency of sulfide oxygenation under visible light irradiation.

Herein we report the synthesis and spectroscopic and electrochemical properties of two new chromophore–catalyst dyads comprising a Ru–aqua complex and its chloro complex. Under visible light irradiation and in the presence of a sacrificial electron acceptor, both complexes exhibited high catalytic activity and product selectivity for photocatalytic oxidation of sulfide into its corresponding sulfoxide in neutral aqueous solution. A PCET process involving formation of a Ru(IV)–oxo intermediate was proposed on the basis of photophysical and electrochemical studies, as well as an isotopic labeling experiment.

EXPERIMENTAL SECTION

Materials and Characterization Methods. $\text{RuCl}_3 \cdot 3\text{H}_2\text{O}$, 4,4'-dimethyl-2,2'-bipyridine, 2-acetylpyridine, $[\text{Co}(\text{NH}_3)_5\text{Cl}]\text{Cl}_2$, 2,2'-bipyridine, NH_4PF_6 , and other chemicals were purchased from Shanghai Energy Chemicals Corp. unless otherwise noted. Standard phosphate buffer solutions at pH 6.8 (0.1 M) were prepared from the sodium phosphate monobasic and dibasic salts ($\text{NaH}_2\text{PO}_4/\text{Na}_2\text{HPO}_4$; Sigma). In pH-dependent experiments, the pH of the sample solutions was finely adjusted by controlled microvolumetric additions of 3.0 M sodium hydroxide or 3.0 M triflic acid solution, and the pH values of the solutions were measured with a pH meter. Organic solvents used in synthetic procedures were of analytical grade and were used without further purification. $\text{Ru}(\text{bpy})_2\text{Cl}_2$, $\text{Ru}(\text{bpy})_3\text{Cl}_2$, $[\text{Ru}(\text{tpy})(\text{bpy})\text{Cl}]\text{Cl}$, and $[\text{Ru}(\text{tpy})(\text{bpy})\text{H}_2\text{O}]\text{Cl}_2$ were synthesized according to literature methods. The purity of each complex was confirmed by ^1H NMR spectroscopy on the basis of the reported data.¹⁴

^1H NMR spectra were recorded on a Bruker Avance 400 spectrometer with chemical shifts (δ , ppm) reported relative to tetramethylsilane. Mass spectra were measured on an APEX II model FT-ICR mass spectrometer. Matrix-assisted laser desorption/ionization time-of-flight (MALDI-TOF) mass spectra were obtained on a Bruker BIFLEX III mass spectrometer. Elemental analyses were performed on a Vario EL III instrument. UV–vis absorption spectra were recorded on a Hitachi U-3010 spectrophotometer. Flash photolysis was carried out on an Edinburgh Instruments LP900 flash photolysis spectrometer. The mixture was excited with 8 ns pulses of a

$\lambda = 355$ nm laser from a frequency-tripled Nd:YAG (neodymium-doped yttrium aluminum garnet) laser device. A single crystal of the ligand **L** was obtained by slow diffusion of diethyl ether into a dichloromethane solution containing **L** at room temperature. Diffraction data were collected on a Rigaku R-Axis RAPID IP X-ray diffractometer using a graphite monochromator with $\text{Mo K}\alpha$ radiation ($\lambda = 0.071073$ nm) at 113 K. The molecular structure of the prepared compound was resolved by direct methods and refined by full-matrix least-squares methods on all F^2 data (SHELXL-97). Non-hydrogen atoms were refined anisotropically. The position of the hydrogen atoms was calculated and refined isotropically.¹⁵ CCDC reference number 987878 contains the supplementary crystallographic data for ligand **L**. These data can be obtained free of charge from The Cambridge Crystallographic Data Centre via www.ccdc.cam.ac.uk/data_request/cif.

Electrochemical measurements were carried out on a CHI660C electrochemical potentiostat. Cyclic voltammetry (CV) and differential pulse voltammetry (DPV) experiments were performed using a three-electrode cell in sodium phosphate buffer. A glassy carbon disk (diameter 3 mm), a platinum plate, and a Ag/AgCl electrode (3 M KCl aqueous solution) were used as the working, counter, and reference electrodes, respectively. The working electrode was successively polished with 3 and 1 μm diamond pastes and sonicated in ion-free water before use. The electrolyte was degassed with nitrogen for 30 min. All potentials are reported vs the normal hydrogen electrode (NHE), and the redox couple $[\text{Ru}(\text{bpy})_3]^{3+}/[\text{Ru}(\text{bpy})_3]^{2+}$, $E_{1/2} = 1.26$ V vs NHE, was used as a standard; the scan rate was 100 mV s^{-1} .

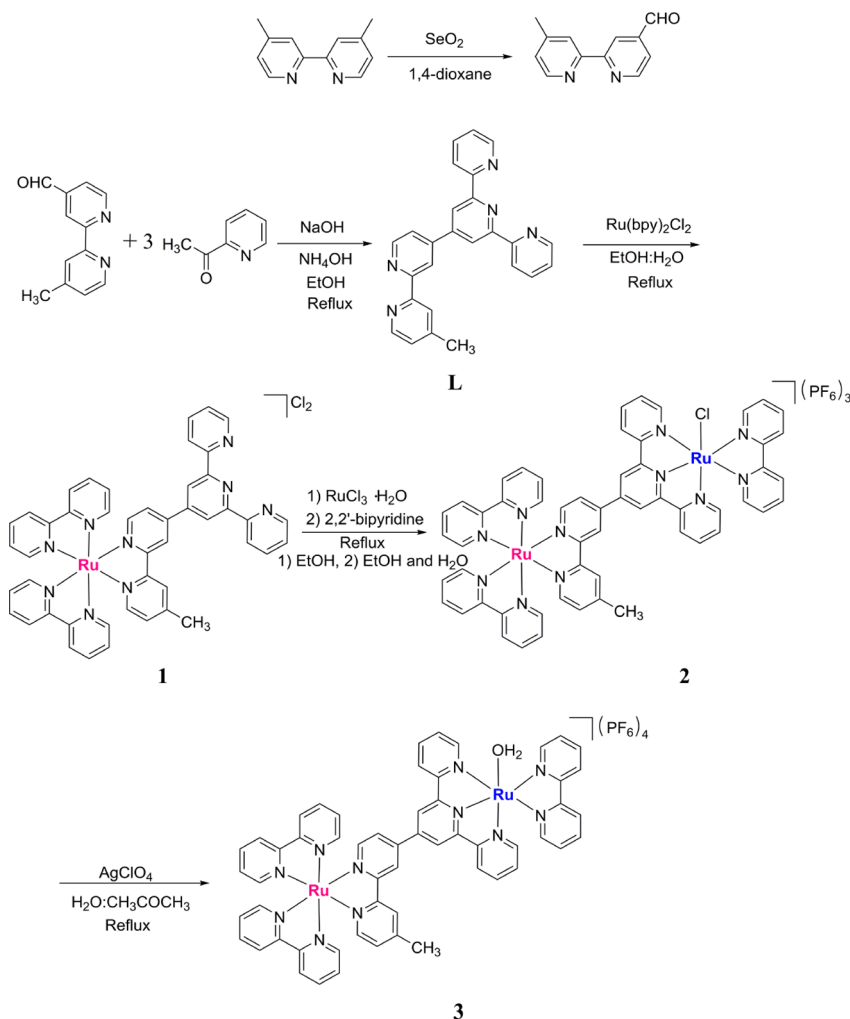
Photocatalytic oxidation of sulfide was investigated in a quartz tube containing the dyad (0.01 mM), the sulfide derivative (10.00 mM), and $[\text{Co}(\text{NH}_3)_5\text{Cl}]\text{Cl}_2$ (20.00 mM) in 0.1 M phosphate buffer (5 mL, pH 6.8). The reaction tube was equipped with a magnetic stirring bar and carefully deaerated with argon for 20 min. The reaction tube was then irradiated by a 3 W white light-emitting diode (LED) light source. After the reaction, the resulting solution was extracted with CH_2Cl_2 (3×10 mL). The combined organic layers were dried over anhydrous sodium sulfate overnight and filtered, and the solvent was removed by rotary evaporation to afford the product. The conversion and turnover number (TON) were determined through ^1H NMR spectroscopy by quantitative analyses of the ratio of integrated peak intensities of the products and the corresponding substrates.

A standard energy meter (Newport model 842) was used for the apparent quantum yield (Φ) determination of photocatalytic oxidation of sulfide. The power of incident monochromatized light of $\lambda = 450$ nm was determined as 60.0 $\text{mW cm}^{-2} \text{ s}^{-1}$, and the irradiated area was confined to 1.0 cm^2 . The 0.1 M phosphate buffer (5 mL, pH 6.8) containing complex **3** (0.01 mM), 4-methoxythioanisole (10.00 mM), and $[\text{Co}(\text{NH}_3)_5\text{Cl}]\text{Cl}_2$ (Co(III); 20.00 mM) was irradiated for 1 h, and the photocatalytic reaction was monitored with a ^1H NMR spectrometer.

The spectroelectrochemical oxidation experiment was conducted on an electrochemical potentiostat and a spectrophotometer. A platinum mesh and a platinum wire were employed as the working electrode and counter electrode, respectively. The Ag/AgCl wire was used as the reference electrode. The three electrodes were immersed in 0.01 mM sample solutions in phosphate-buffered saline (PBS) in an electrochemical vessel with an optical cell of 1.0 cm optical path length. This system was loaded with a 1.0 V vs NHE potentiostatic voltage for 2.0 min, and the spectral changes were monitored by UV–vis absorption spectroscopy simultaneously.

Synthesis of Ligand **L (tpy–bpy).** 4-Methyl-2,2'-bipyridine-4'-carbaldehyde was obtained by reacting 4,4'-dimethyl-2,2'-bipyridine and selenium dioxide in refluxing 1,4-dioxane with stirring for 4 h under a nitrogen atmosphere. 4-Methyl-2,2'-bipyridine-4'-carbaldehyde (400 mg, 2.01 mmol), 2-acetylpyridine (752 mg, 6.02 mmol), and aqueous NH_3 (10 mL, 12.04 mmol) were dissolved in ethanol (50 mL). NaOH (240 mg, 6.00 mmol) was added to the solution, which was then heated at reflux for 48 h. After being cooled to room temperature, the resulting brown solution was kept in a refrigerator. After 12 h a residue was collected by filtration and washed with water

Scheme 1. Synthesis of the Chromophore-Catalyst Supramolecules



(50 mL) followed by cold EtOH (50 mL). The precipitate was purified by column chromatography using silica gel and dichloromethane/methanol (70:1, v/v) as the eluent. The solvent was evaporated to give **L** as a white solid (300 mg, 75% yield). MALDI-TOF-MS (m/z): calcd 402.2 $[\text{M} + \text{H}]^+$, found 402.2; calcd 424.2 $[\text{M} + \text{Na}]^+$, found 424.2. ^1H NMR (400 MHz, CDCl_3): δ (ppm) 8.90 (d, 1H, $J = 1.0$ Hz), 8.86 (s, 2H), 8.82 (d, 1H, $J = 5.1$ Hz), 8.74 (d, 2H, $J = 4.0$ Hz), 8.68 (d, 2H, $J = 7.9$ Hz), 8.60 (d, 1H, $J = 4.9$ Hz), 8.31 (s, 1H), 7.89 (td, 2H, $J = 7.8, 1.7$ Hz), 7.80 (dd, 1H, $J = 5.0, 1.0$ Hz), 7.37 (td, 2H, $J = 4.9, 1.8$ Hz), 7.18 (d, 1H, $J = 4.8$ Hz), 2.48 (s, 3H). ^{13}C NMR (101 MHz, CDCl_3): δ (ppm) 158.1, 157.2, 156.7, 156.5, 150.7, 150.1, 150.0, 149.1, 148.8, 148.1, 137.8, 125.9, 124.9, 123.1, 122.6, 122.3, 120.2, 119.9, 22.1.

Synthesis of Complex 1 ($\text{Ru}_{\text{phot}}\text{-tpy}$). $\text{Ru}(\text{bpy})_2\text{Cl}_2$ (120 mg, 0.25 mmol) was added to a solution of ligand **L** (100 mg, 0.25 mmol) in an ethanol-water solution (20 mL; 1:1, v/v). The resulting solution was degassed for 15 min by argon bubbling and then refluxed for 5 h. A red precipitate was collected by filtration from the hot solution. This material was dissolved in a minimum volume of water and reprecipitated by the addition of excess NH_4PF_6 . After filtration, complex **1** was obtained as a red powder (80 mg, 66% yield). Electrospray ionization mass spectrometry (ESI-MS; m/z): calcd 407.6 $[\text{M} - 2(\text{PF}_6)]^{2+}$, found 407.6. ^1H NMR (400 MHz, $\text{DMSO}-d_6$): δ (ppm) 9.30 (s, 1H), 9.13 (s, 1H), 8.86 (t, 6H, $J = 10.7$ Hz), 8.77 (d, 2H, $J = 4.2$ Hz), 8.71 (d, 2H, $J = 8.0$ Hz), 8.19 (dd, 4H, $J = 14.6, 7.7$ Hz), 8.08 (td, 2H, $J = 7.7, 1.6$ Hz), 8.00 (dd, 1H, $J = 6.0, 1.6$ Hz), 7.88 (d, 1H, $J = 5.6$ Hz), 7.85 (d, 1H, $J = 6.0$ Hz), 7.79 (t, 2H, $J = 6.1$ Hz), 7.76 (d, 1H, $J = 5.4$ Hz), 7.61 (d, 1H, $J = 5.8$ Hz), 7.56 (m, 6H), 7.42 (d, 1H, $J = 5.6$ Hz), 2.56 (s, 3H). ^{13}C NMR (101 MHz, $\text{DMSO}-d_6$): δ

(ppm): 158.2, 157.3, 157.2, 157.1, 156.8, 156.5, 155.1, 152.3, 152.0, 151.9, 151.7, 150.9, 150.5, 150.0, 147.2, 146.6, 138.5, 138.3, 129.5, 128.5, 126.6, 125.5, 125.3, 125.2, 125.0, 122.9, 121.8, 119.5, 21.3.

Synthesis of Supramolecule 2 ($\text{Ru}_{\text{phot}}\text{-Ru}_{\text{cat}}\text{-Cl}$). Complex **1** (600 mg, 0.70 mmol) and $\text{RuCl}_3 \cdot 3\text{H}_2\text{O}$ (200 mg, 0.70 mmol) were dissolved in ethanol (20 mL). The resulting solution was refluxed for 5 h. After the solution was cooled to room temperature, the solvent was removed by rotary evaporation, and the resulting brown solid was dissolved in an ethanol/ H_2O solution (30 mL; 3:1, v/v) followed by the addition of 2,2'-bipyridine (bpy) (124.2 mg, 0.80 mmol), LiCl (170 mg, 4.00 mmol), and triethylamine (0.20 mL). The solution was degassed by argon bubbling and heated at reflux for 12 h. The hot mixture was filtered, and the solvent volume was reduced by rotary evaporation. The complex was precipitated by the addition of excess NH_4PF_6 and filtered. The crude product was purified by column chromatography using silica gel and a mixture of acetonitrile/saturated KNO_3 aqueous solution (20:1, v/v) as the eluent to give a red solid; this solid was dissolved in a minimum volume of water and reprecipitated by the addition of excess NH_4PF_6 to give **2** (210 mg, 60% yield). HR-ESI-MS (m/z): calcd 1398.0762 $[\text{M} - \text{PF}_6]^+$, found 1398.0798; calcd 626.5560 $[\text{M} - 2(\text{PF}_6)]^{2+}$, found 626.5554; calcd 369.3826 $[\text{M} - 3(\text{PF}_6)]^{3+}$, found 369.0458. ^1H NMR (400 MHz, CD_3CN): δ (ppm) 10.21 (d, 1H, $J = 4.9$ Hz), 9.11 (d, 1H, $J = 1.7$ Hz), 8.88 (s, 2H), 8.76 (s, 1H), 8.63 (d, 1H, $J = 8.2$ Hz), 8.56 (m, 6H), 8.31 (m, 2H), 8.09 (m, 5H), 7.99 (m, 2H), 7.92 (m, 3H), 7.81 (d, 2H, $J = 5.6$ Hz), 7.77 (d, 1H, $J = 5.0$ Hz), 7.70 (d, 3H, $J = 6.2$ Hz), 7.63 (d, 1H, $J = 5.8$ Hz), 7.46 (m, 4H), 7.32 (m, 4H), 6.94 (t, 1H, $J = 7.2$ Hz), 2.62 (s, 3H). Anal. Calcd for $\text{C}_{56}\text{H}_{43}\text{ClF}_{18}\text{N}_{11}\text{P}_3\text{Ru}_2 \cdot 1.5\text{H}_2\text{O}$: C, 42.85; H, 2.95; N, 9.82. Found: C, 42.68; H, 2.82; N, 9.65.

Synthesis of Supramolecule 3 (Ru_{phot}–Ru_{cat}–H₂O). Complex 2 (50 mg, 0.041 mmol) and AgClO₄ (90 mg, 0.41 mmol) were dispersed in a water/acetone solution (30 mL; 4:1, v/v) and heated at reflux for 12 h in the dark under an argon atmosphere. After the solution was cooled to room temperature, the white solid AgCl was filtrated, and the filtrate was concentrated in vacuum. Addition of excess NH₄PF₆ led to precipitation of a red solid. The crude product was recrystallized from diethyl ether to give a deep red solid (33 mg, 66% yield). HR-ESI-MS (*m/z*): calcd 1382.1112 [M – 2(PF₆) – H]⁺, found 1382.1079; calcd 618.0768 [M – 3(PF₆) – H]²⁺, found 618.0717. ¹H NMR (400 MHz, (CD₃)₂CO): δ (ppm) 9.74 (d, 1H, *J* = 5.1 Hz), 9.35 (d, 1H, *J* = 1.4 Hz), 9.15 (d, 2H, *J* = 3.4 Hz), 8.98 (s, 1H), 8.81 (dd, 2H, *J* = 8.1, 3.2 Hz), 8.77 (d, 1H, *J* = 8.2 Hz), 8.68 (t, 4H, *J* = 8.0 Hz), 8.48 (m, 2H), 8.21 (m, 6H), 8.13 (m, 3H), 8.04 (d, 1H, *J* = 5.4 Hz), 7.94 (m, 3H), 7.87 (d, 1H, *J* = 5.1 Hz), 7.84 (d, 2H, *J* = 5.4 Hz), 7.74 (d, 1H, *J* = 5.8 Hz), 7.55 (m, 6H), 7.45 (d, 2H, *J* = 5.8 Hz), 7.20 (t, 1H, *J* = 6.1 Hz), 6.05 (s, 2H), 2.74 (s, 3H). Anal. Calcd for C₃₆H₄₃F₂₄N₁₁OP₄Ru₂·2H₂O: C, 40.27; H, 2.72; N, 9.23. Found: C, 39.89; H, 2.52; N, 8.89.

RESULTS AND DISCUSSION

Synthesis, Characterization, and Structure. The synthetic route for supramolecules is shown in Scheme 1. First, the monometallic complex 1 was prepared by refluxing Ru(bpy)₂Cl₂ with the bridging tpy–bpy ligand L. This complex was reacted further with RuCl₃·3H₂O to generate a dinuclear intermediate, which was treated with 1 equiv of bpy to afford Ru_{phot}–Ru_{cat}–Cl with three Cl[–] anions. Finally, the complex was purified on silica gel and then converted to the PF₆[–] salt by addition of excess NH₄PF₆ in moderate yield. The complex Ru_{phot}–Ru_{cat}–H₂O was obtained by directly reacting the chloro complex with AgClO₄ in aqueous solution at reflux.¹⁶ Dinuclear complexes 2 and 3 were characterized by ¹H NMR spectroscopy, high-resolution mass spectrometry, and elemental analysis. Complex 2 showed one distinct doublet at low field (δ ≈ 10.21 ppm), which was assigned to the bpy proton closest to the chloro ligand. In the case of complex 3, this doublet was shifted upfield (δ ≈ 9.74 ppm) due to the larger diamagnetic anisotropy of the aqua ligand.¹⁷ The presence of H₂O as a ligand in complex 3 was demonstrated by a ¹H NMR spectroscopy exchange experiment. The singlet signal at 6.05 ppm measured in acetone-*d*₆ disappeared immediately after addition of 0.1 mL of D₂O, suggesting the existence of H₂O/D₂O exchange. The mass spectrum of the chloro complex 2 displayed a single-charge ion at *m/z* = 1398.0798, which was ascribed to [2 – PF₆]⁺, the another two ESI-MS signals at *m/z* = 626.5554 and 369.0458 that could be assigned to [2 – 2(PF₆)]²⁺ and [2 – 3(PF₆)]³⁺, respectively. The mass spectrum of complex 3 showed an ESI-MS signal at *m/z* = 1382.1079, which was consistent with the tetracation plus two PF₆[–] ions minus one H⁺ ion. A single crystal of ligand L was obtained by slow diffusion of diethyl ether into dichloromethane solution containing L at room temperature. The corresponding molecular structure is shown in Figure 1. Detailed crystal data are listed in Table S1 (Supporting Information).

Spectroscopic Properties. The absorption properties of complexes 2 and 3 in phosphate buffer at pH 6.8 were investigated, and the data are listed in Table 1. As shown in Figure 2, Ru_{phot}–Ru_{cat}–Cl displayed strong and broad absorption bands in the visible light region with λ_{max} at 470 and 525 nm, attributed to metal-to-ligand charge transfer (MLCT) transitions of the Ru_{phot} moiety and Ru_{cat}–Cl unit, respectively.¹⁸ The MLCT absorptions originating from Ru_{phot} and Ru_{cat}–Cl moieties in Ru_{phot}–Ru_{cat}–Cl are separated in

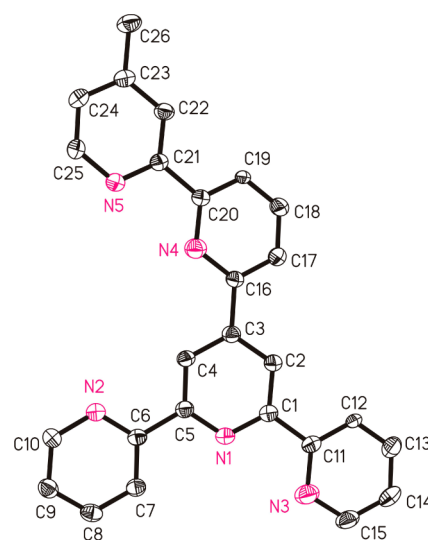


Figure 1. Perspective view and labeling scheme for ligand L with thermal ellipsoids at 30% probability. Hydrogen atoms are omitted for clarity.

energy. This suggests that the extinction coefficient of the MLCT for the assembly is almost the sum of the MLCT molar absorptions for Ru_{phot} and Ru_{cat}–Cl species and indicates weak electronic coupling between the two metal sites in complex 2. Therefore, high electron injection efficiencies from the catalytic center to the chromophore fragment may be expected, as well as diminished excited-state electron recombination. However, it should be noted that the weak electronic coupling between the Ru_{phot} and Ru_{cat} shifts the position of the MLCT transition absorption for two moieties compared with their corresponding mononuclear complexes (Table 1), whereas the UV–vis absorption spectra of Ru_{phot}–Ru_{cat}–H₂O displayed one MLCT absorption with λ_{max} at 495 nm, which corresponds with the overlapping MLCT band of the Ru_{phot} and Ru_{cat}–H₂O fragments. Additionally, the lowest energy band shifts to a shorter wavelength when the Cl[–] ligand in complex 2 is displaced by H₂O to form a Ru–aqua complex. This is caused by the absence of a π-donation effect from the Cl[–] ligand and increases the HOMO–LUMO energy gap.¹⁹ The two complexes showed negligible emission, and their emission lifetimes were shorter than 1 ns, in contrast to the mononuclear complex 1, which exhibits intense emission with a λ_{max} at 630 nm. This weak emission can be attributed to quenching of the excited state of the Ru_{phot} site by the Ru_{cat} unit.

The time-resolved absorption difference spectra of complex 3 were recorded following flash photolysis at 355 nm. As depicted in Figure 3, the spectra showed absorption peaks at about 385 and 590 nm (τ = 73 ns). However, in the presence of electron acceptor Co(III), the signal intensities are below the resolution of our detection system, and the excited-state lifetime was reduced to 41 ns (Figure S12, Supporting Information), indicating addition of excess Co(III) promoted an intramolecular electron transfer from Ru_{cat} to *Ru_{phot} through the intermolecular interaction.^{16,19}

Electrochemical Properties. The redox potentials of complexes 2 and 3 in aqueous phosphate buffer were investigated by CV and DPV, and the results are listed in Table 1. CV of the chloro dinuclear complex Ru_{phot}–Ru_{cat}–Cl (Figure S13, Supporting Information) in phosphate buffer (0.1 M, pH 6.8) exhibited one reversible redox process at 1.00 V

Table 1. Spectroscopic Data and Electrochemical Results for Complexes 2 and 3 and Their Mononuclear Moieties in 0.1 M Aqueous Phosphate Buffer at pH 6.8

compd	λ_{\max}/nm ($\epsilon/M^{-1}\text{cm}^{-1}$)		$E_{1/2}^a/\text{V}$ vs NHE (ΔE)	
	$\pi\pi^*$	$d\pi_{\text{Ru(phot or cat)}}\pi^*$	$\text{Ru(III/II,IV/III)}_{\text{cat}}$	$\text{Ru(III/II)}_{\text{phot}}$
$[\text{Ru}(\text{bpy})_3]^{2+}$	290 (88000)	420 (13000) 465 (17000)		1.26 (60)
$[\text{Ru}(\text{bpy})(\text{tpy})\text{Cl}]^+$	290 (48000)	500 (10000)	1.00 (58)	
$[\text{Ru}(\text{bpy})(\text{tpy})\text{H}_2\text{O}]^{2+}$	290 (41000) 320 (41000)	480 (11000)	0.75 (53), 0.80 (52)	
$\text{Ru}_{\text{phot}}-\text{Ru}_{\text{cat}}-\text{Cl}$	290 (90000)	470 (18000) 525 (18500)	1.00 (71)	1.32 (63)
$\text{Ru}_{\text{phot}}-\text{Ru}_{\text{cat}}-\text{H}_2\text{O}$	290 (108000)	495 (22000)	0.77 (110)	1.32 (65)

^a $E_{1/2} = (E_{\text{ox}} + E_{\text{red}})/2$ in volts, and $\Delta E = E_{\text{ox}} - E_{\text{red}}$ in millivolts.

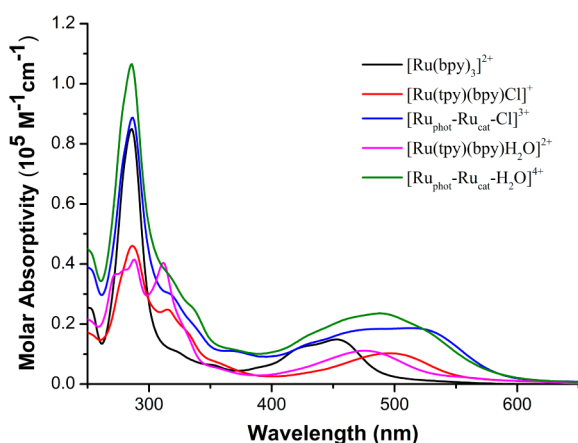


Figure 2. Absorption spectra for $[\text{Ru}(\text{bpy})_3]^{2+}$, $[\text{Ru}(\text{tpy})(\text{bpy})\text{Cl}]^+$, $\text{Ru}_{\text{phot}}-\text{Ru}_{\text{cat}}-\text{Cl}$, $[\text{Ru}(\text{tpy})(\text{bpy})\text{H}_2\text{O}]^{2+}$, and $\text{Ru}_{\text{phot}}-\text{Ru}_{\text{cat}}-\text{H}_2\text{O}$ in 0.1 M aqueous phosphate buffer at pH 6.8 and room temperature.

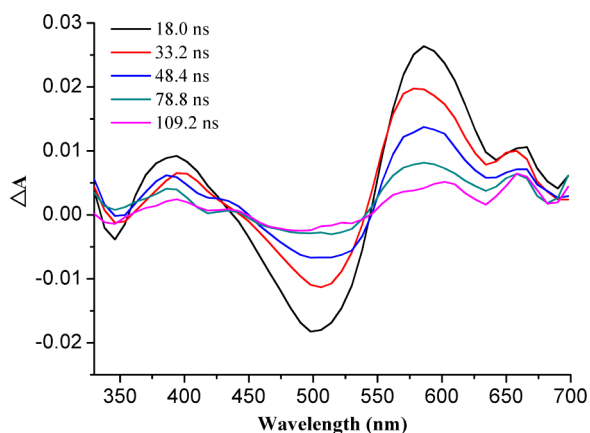


Figure 3. Transient absorption spectra of complex 3 in phosphate buffer (0.1 M, pH 6.8) under an argon atmosphere with an 8 ns laser pulse at 355 nm.

and one quasi-reversible redox course at 1.32 V vs NHE. In comparison, the redox potentials of complex 2 are similar to those of its corresponding mononuclear fragments $[\text{Ru}(\text{tpy})(\text{bpy})\text{Cl}]^+$ (1.00 V) and $[\text{Ru}(\text{bpy})_3]^{2+}$ (1.26 V).²⁰ Previous investigations reported by Rocha and his colleagues have found that substitution of the tpy–tpy bridging ligand by a more conjugated bridging backbone 2,3,5,6-tetrakis(2-pyridyl)pyrazine results in charge delocalization across the bridging ligand and thus lowers the photocatalytic efficiency.²¹ In the

present work, the single bond of the tpy–bpy bridge reduces charge trapping between the Ru_{phot} and Ru_{cat} centers. CV of the aqua complex 3 showed two apparently reversible redox processes at 0.77 and 1.32 V in aqueous solution. As shown in Figure 4, the redox occurring at 1.32 V is ascribed to the

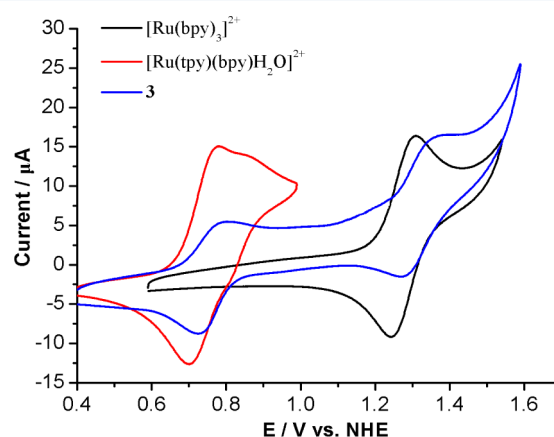


Figure 4. Cyclic voltammograms of $[\text{Ru}(\text{bpy})_3]^{2+}$ (black), $[\text{Ru}(\text{tpy})(\text{bpy})\text{H}_2\text{O}]^{2+}$ (red), and complex 3 (blue) in 0.1 M aqueous phosphate buffer (pH 6.8) at 25 °C. The data were recorded at a scan rate of 100 mV s^{-1} in air.

$\text{Ru(II)}/\text{Ru(III)}$ redox course of the Ru_{phot} center, while the mononuclear $[\text{Ru}(\text{tpy})(\text{bpy})\text{H}_2\text{O}]^{2+}$ species displayed two successive redox courses at 0.75 and 0.80 V under the same conditions which are assigned to two PCET processes of $\text{Ru(II)}-\text{OH}_2/\text{Ru(III)}-\text{OH}$ and $\text{Ru(III)}-\text{OH}/\text{Ru(IV)}=\text{O}$, respectively.^{12,22} The different electrochemical behavior of the Ru_{cat} site in complex 3 may be caused by the overlap of two one-electron redox processes with an average potential of 0.77 V. To gain further insight into the redox process at the Ru_{cat} site in complex 3, we measured the pH dependence of the potentials for complex 3 in aqueous solution for pH values ranging from 1.0 to 13.0 (Figure S14, Supporting Information). The Pourbaix diagram for complex 3 shows that the two consecutive PCET processes followed well-defined lines with the slope close to -59 mV per pH unit over the range of pH 2–11, ascribed to two $1e^-/1\text{H}^+$ PCET processes of $\text{Ru(II)}-\text{OH}_2/\text{Ru(III)}-\text{OH}$ and $\text{Ru(III)}-\text{OH}/\text{Ru(IV)}=\text{O}$ redox couples. The narrow $E_{1/2}$ separations indicate a very efficient redox potential leveling in this catalyst. Moreover, the $\text{Ru(II)}/\text{Ru(III)}$ oxidation of the Ru_{phot} center is pH-independent.¹⁴ Figure 4 shows that intramolecular electron transfer from $\text{Ru}_{\text{cat}}-\text{H}_2\text{O}$ to the photogenerated $\text{Ru(III)}_{\text{phot}}$ moiety in 3, with

a driving force of 550 mV, would be thermodynamically favorable in water via PCET processes. In contrast, because there is no PCET process involved, even though the Cl⁻ ligand is a strong π -electron donor, the oxidation potential of Ru(III)_{cat}/Ru(II)_{cat} in Ru_{phot}-Ru_{cat}-Cl is higher than that of the Ru(II)-OH₂/Ru(IV)=O couple for its aqua complex (Table 1).²³

Photooxidation of Sulfide. Light-driven oxidation of sulfide was performed using Co(III)²⁴ as a sacrificial electron acceptor in deoxygenated phosphate buffer (0.1 M, pH 6.8) with a complex (2 or 3):substrate:Co(III) mole ratio of 1:1000:2000 under white LED irradiation ($\lambda > 380$ nm) at room temperature. The corresponding products were extracted with dichloromethane and studied by ¹H NMR spectroscopy. In the presence of a 4-methoxythioanisole substrate, the sulfide was oxidized into the corresponding sulfoxide with 99% product selectivity and a TON of up to 709 was achieved on the basis of Ru_{phot}-Ru_{cat}-H₂O after 8 h of irradiation. Ru_{phot}-Ru_{cat}-Cl is the precatalyst, and it would convert to its aqua form by a fast Cl⁻/H₂O ligand exchange to achieve a lower efficiency with a TON of 645 under the same conditions, as shown in Figures 5

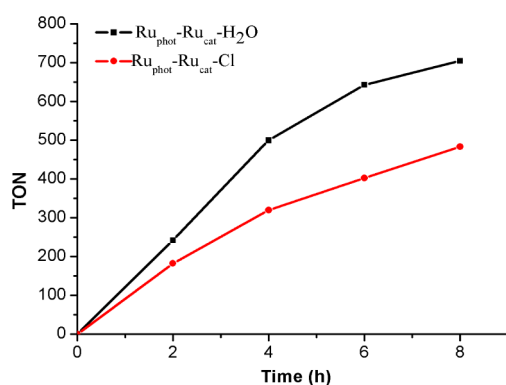


Figure 5. Turnover number for the photocatalytic oxidation of 4-methoxythioanisole by 2 (red) and 3 (black) under argon as a function of the irradiation time.

and 6. The efficiency of the catalytic photooxidation of sulfide in a solution containing [Ru(bpy)₃]²⁺ (0.01 mM), [Ru(tpy)-(bpy)H₂O]²⁺ (0.01 mM), 4-methoxythioanisole (10 mM), and Co(III) (20 mM) was markedly lower (with a TON of only 101 after 8 h) compared with that of the supramolecular system at identical reaction conditions. This indicates that the

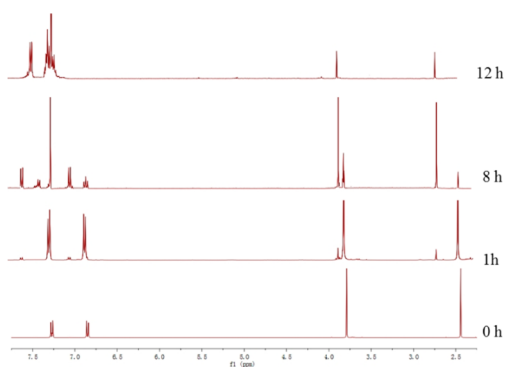
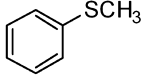
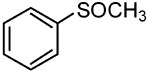
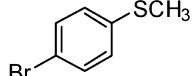
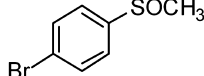
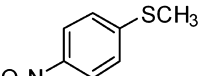
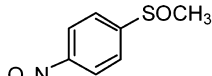
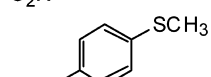
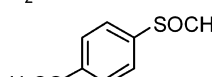
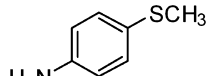
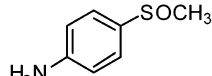


Figure 6. ¹H NMR (CDCl₃) spectra of the substrate (4-methoxythioanisole) and product using 3 as the photocatalyst in the photooxidation reaction at different reaction times.

supramolecular assembly exhibits superior photocatalytic activity compared with a multicomponent system. Additionally, control experiments confirmed that light, complex, and sacrificial electron acceptors are necessary for photooxidation of sulfide. Notably, when an additional 20 mM Co(III) was added to the Ru_{phot}-Ru_{cat}-H₂O system after reaction for 8 h, the resulting solution was irradiated for another 4 h and the TON increased to nearly 1000. This highlights the excellent photostability of the catalysts. Moreover, we measured the apparent quantum yield (Φ) of this reaction. The phosphate buffer (0.1 M, 5 mL, pH 6.8) containing complex 3 (0.01 mM), 4-methoxythioanisole (10.00 mM), and Co(III) (20.00 mM) was irradiated by monochromatized light of $\lambda = 450$ nm (the power of the light is 60.0 mW cm⁻² s⁻¹) for 1 h, a TON of 60 was achieved, and the apparent quantum yield was determined to be 0.7% by monitoring the formation of the product with ¹H NMR spectroscopy. Different substrates were also used to study the scope of photocatalytic activities of both complexes. The results are summarized in Table 2. All the sulfides were converted into their corresponding sulfoxides without formation of sulfones. Substrates bearing electron-donating groups gave better results than those bearing electron-withdrawing groups, suggesting an electronic effect. The photooxidation of a sulfide bearing a -NH₂ substituent could be achieved in higher TON than that of a sulfide bearing a -NO₂ group for both catalysts Ru_{phot}-Ru_{cat}-H₂O and Ru_{phot}-Ru_{cat}-Cl.

Mechanistic Interpretation. Inspired by the high efficiency of the present system, we were motivated to study the catalytic mechanism. The changes in species following electrochemical oxidation of Ru(II)_{phot}-Ru(II)_{cat}-H₂O at an applied potential of 1.0 V were monitored by UV-vis absorption spectra. As shown in Figure 7, the MLCT band with λ_{max} at 495 nm originating from the complex Ru_{phot}-Ru_{cat}-H₂O blue-shifted to 490 nm, and the absorption band with λ_{max} at 522 nm ascribed to an MLCT transition of the Ru_{cat} moiety in 3 disappeared during the electrochemical reaction. A comparison of the spectral data for MLCT bands in Table 1 and Figure 7 indicates that oxidation of the Ru_{cat}-OH₂ unit into Ru(III)_{cat}-OH/Ru(IV)_{cat}=O occurred through application of a 1.0 V potential.^{21a} The remaining λ_{max} at 490 nm is assigned to the MLCT excitation of the Ru_{phot} moiety. Moreover, this behavior was clearly observed for Ru_{phot}-Ru_{cat}-Cl, as shown in Figure S15 (Supporting Information). Upon irradiation of an aqueous solution containing Ru_{phot}-Ru_{cat}-OH₂ and excess Co(III), we found that the intensity of the MLCT absorption at 522 nm, ascribed to Ru(II)_{cat}-OH₂, declined and that of the Ru(II)_{phot} unit became more obvious, indicating that a photoinduced electron transfer from Ru(II)_{cat}-OH₂ to Ru(III)_{phot} occurred. The presence of the Ru(IV)=O intermediate was detected by HR-ESI mass spectra in our previous work under the same conditions.^{11b} Furthermore, the initial MLCT absorption band of Ru(II)_{phot}-Ru(II)_{cat}-H₂O could be recovered on addition of 4-methoxythioanisole to the above solution under dark conditions, caused by electron transfer from sulfide to Ru(IV)=O (Figures S16 and S17, Supporting Information). An investigation into the role of H₂O in the photocatalytic reaction can help us to further understand the mechanistic nature of this PCET process. An isotopic labeling experiment was conducted using a 2:1 mixture of H₂¹⁶O and H₂¹⁸O as the solvent and 4-methoxythioanisole as the substrate. The products of photocatalytic oxidation after irradiation for 8 h were extracted by dichloromethane, and the solvent was

Table 2. Photocatalytic Oxidation of Sulfide Using Complex 3 in Phosphate Buffer^a

Substrate	Product	TON (sel. [%])	
		Ru _{phot} -Ru _{cat} -Cl	Ru _{phot} -Ru _{cat} -H ₂ O
		532 (99)	745 (99)
		237 (99)	314 (99)
		167 (99)	265 (99)
		645 (99)	709 (99) 1000 (99) ^b
		512 (99)	567 (99)

^aConditions: [cat] = 0.01 mM, [substrate] = 10 mM, [Co(III)] = 20 mM; the reaction was processed in 0.1 M phosphate buffer (pH 6.8) for 8 h under an argon atmosphere using an LED ($\lambda > 380$ nm) as the light source. ^bAddition of another 20 mM Co(III) into the reaction solution and illumination for a further 4 h.

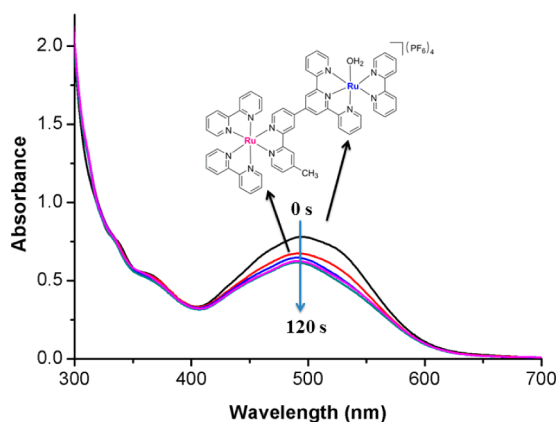


Figure 7. Changes of visible absorption spectra following the spectroelectrochemical oxidation of Ru(II)_{phot}-Ru(II)_{cat}-H₂O (black) into its Ru(II)_{phot}-Ru(IV)_{cat}=O intermediate by applying a potential of 1.0 V over 120 s.

removed by rotary evaporation. The obtained product was characterized by ESI-MS. The mass spectra (Figure 8; Figure S18, Supporting Information) displayed two peaks: one at 193.0292 [M + Na]⁺ with fragments at 194.0307 and 195.1731 and [M* + Na]⁺ at 195.0610 with fragments at 196.0724 and 197.0699, assigned to a 2:1 mixture of unlabeled and labeled sulfoxides. These results confirm that water is the oxygen source for the photooxidation reaction of the organic substrate and that a PCET process occurs. On the basis of previous reports and these results, a proposed catalytic mechanism is presented in Scheme 2.^{3a,12,25} The excited-state *Ru(II)_{phot} moiety can be quenched by the sacrificial electron acceptor Co(III), which provides a driving force for oxidizing the neighboring Ru(II)_{cat}-H₂O moiety to generate Ru(IV)=O species through subsequent PCET processes. However, a mechanism involving successive two-electron two-proton oxidation processes cannot be entirely ruled out because an overlapping two-electron electrocatalytic oxidation process for

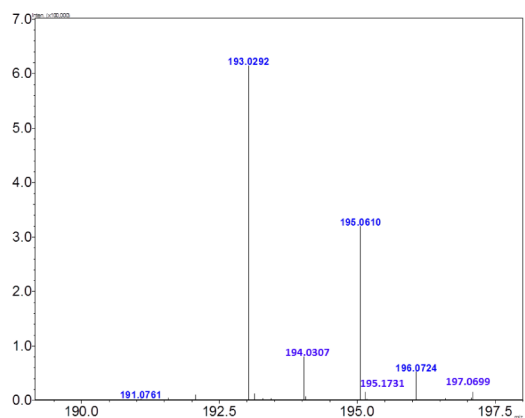
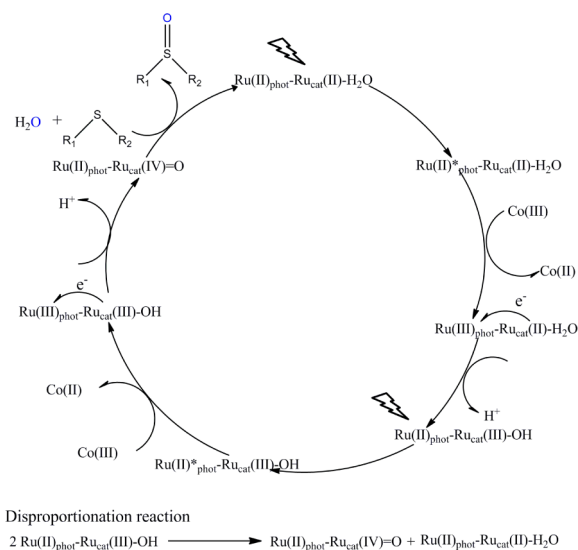


Figure 8. Corresponding labeled and unlabeled sulfoxide obtained in an unbuffered degassed H₂¹⁶O/H₂¹⁸O (2:1) mixture. The fragments at *m/z* 193.0292, 194.0307, and 195.1731 are assigned to unlabeled sulfoxide plus one Na⁺ adduct. The fragments at *m/z* 195.0610, 196.0724, and 197.0699 are assigned to labeled sulfoxide plus one Na⁺ adduct.

the Ru(II)_{cat}-H₂O moiety was observed in CV experiments. The generated Ru(IV)=O species is considered to be the active intermediate for the oxygenation of sulfide to the corresponding sulfoxide with high efficiency and selectivity.^{11e,f}

In conclusion, we have synthesized two new and structurally simple chromophore-catalyst dyads, Ru_{phot}-Ru_{cat}-Cl and Ru_{phot}-Ru_{cat}-H₂O. The single bond in the tpy-bpy bridging ligand decreases charge trapping at the linker between the Ru_{phot} and Ru_{cat} sites. Both complexes showed remarkable visible-light-driven catalytic activities with TONs of up to 1000 (Ru_{phot}-Ru_{cat}-H₂O) and high product selectivity (>99%) toward oxidation of sulfide to the corresponding sulfoxide in neutral aqueous solution. Spectroscopic and electrochemical investigations revealed an excited-state *Ru(II)_{phot} moiety initiates the PCET process, which results in the formation of an active Ru(IV)_{cat}=O intermediate in the presence of one-

Scheme 2. Proposed Mechanism for Photocatalytic Oxygenation of Sulfides



electron acceptor Co(III). An isotopic labeling experiment showed that water is the source of oxygen in the organic substrates following photooxidation. These results have important consequences for the photocatalytic oxidation of substrates by related dyad catalysts and add a new dimension to the understanding of PCET mechanisms.

■ ASSOCIATED CONTENT

● Supporting Information

X-ray crystallographic data for ligand **L** in CIF format, NMR spectra of the compounds, electronic absorption and HR-ESI mass spectra of the complexes, results of electrochemical studies, and photocatalytic oxygenation results. This material is available free of charge via the Internet at <http://pubs.acs.org>.

■ AUTHOR INFORMATION

Corresponding Author

*E-mail: fuwf@mail.ipc.ac.cn.

Notes

The authors declare no competing financial interest.

■ ACKNOWLEDGMENTS

This work was supported by the National Key Basic Research Program of China (973 Program 2013CB834804) and by the Ministry of Science and Technology of China (Grant 2012DFH40090). We thank the National Natural Science Foundation of China (NSFC Grants 21267025, 21273257, 21367026, and U1137606) for financial support.

■ REFERENCES

- (1) (a) Narayanam, J. M. R.; Stephenson, C. R. J. *Chem. Soc. Rev.* **2011**, *40*, 102–113. (b) Inagaki, A.; Akita, M. *Coord. Chem. Rev.* **2010**, *254*, 1220–1239. (c) Fagnoni, M.; Dondi, D.; Ravelli, D.; Albini, A. *Chem. Rev.* **2007**, *107*, 2725–2756. (d) Sun, L.; Hammarström, L.; Akermark, B.; Styring, S. *Chem. Soc. Rev.* **2001**, *30*, 36–49. (e) Lewis, N. S.; Nocera, D. G. *Proc. Natl. Acad. Sci. U.S.A.* **2006**, *103*, 15729–15735. (f) Wasielewski, M. R. *Acc. Chem. Res.* **2009**, *42*, 1910–1921.
- (2) (a) Renger, G. *Photosynth. Res.* **2007**, *92*, 407–425. (b) Ferreira, K. N.; Iverson, T. M.; Maghlaoui, K.; Barber, J.; Iwata, S. *Science* **2004**, *303*, 1831–1838. (c) Zouni, A.; Witt, H. T.; Kern, J.; Fromme, P.; Kraus, N.; Saenger, W.; Orth, P. *Nature* **2001**, *409*, 739–742.

(d) Umena, Y.; Kawakami, K.; Shen, J.-R.; Kamiya, R. N. *Nature* **2011**, *473*, 55–60.

(3) (a) Fukuzumi, S.; Kishi, T.; Kotani, H.; Lee, Y.-M.; Nam, W. *Nat. Chem.* **2011**, *3*, 38–41. (b) Concepcion, J. J.; Jurss, J. W.; Brenneman, M. K.; Hoertz, P. G.; Patrocino, A. O. T.; Murakami Iha, N. Y.; Templeton, J. L.; Meyer, T. J. *Acc. Chem. Res.* **2009**, *42*, 1954–1965. (c) Zeitler, K. *Angew. Chem., Int. Ed.* **2009**, *48*, 9785–9789. (d) Ashford, D. L.; Stewart, D. J.; Glasson, C. R.; Binstead, R. A.; Harrison, D. P.; Norris, M. R.; Concepcion, J. J.; Fang, Z.; Templeton, J. L.; Meyer, T. J. *Inorg. Chem.* **2012**, *51*, 6428–6430.

(4) (a) Sono, M.; Roach, M. P.; Coulter, E. D.; Dawson, J. H. *Chem. Rev.* **1996**, *96*, 2841–2888. (b) Meunier, B.; de Visser, S. P.; Shaik, S. *Chem. Rev.* **2004**, *104*, 3947–3980. (c) Gunay, A.; Theopold, K. H. *Chem. Rev.* **2010**, *110*, 1060–1081. (d) Meyer, T. J.; Huynh, M. H. V. *Inorg. Chem.* **2003**, *42*, 8140–8160. (e) Moonshiram, D.; Alperovich, I.; Concepcion, J. J.; Meyer, T. J.; Pushkar, Y. *Proc. Natl. Acad. Sci. U.S.A.* **2013**, *110*, 3765–3770. (f) Hirai, Y.; Kojima, T.; Mizutani, Y.; Shiota, Y.; Yoshizawa, K.; Fukuzumi, S. *Angew. Chem., Int. Ed.* **2008**, *47*, 5772–5776. (g) Kojima, T.; Nakayama, K.; Ikemura, K.; Ogura, T.; Fukuzumi, S. *J. Am. Chem. Soc.* **2011**, *133*, 11692–11700.

(5) (a) Low, D. W.; Winkler, J. R.; Gray, H. B. *J. Am. Chem. Soc.* **1996**, *118*, 117–120. (b) Berglund, J.; Pascher, T.; Winkler, J. R.; Gray, H. B. *J. Am. Chem. Soc.* **1997**, *119*, 2464–2469.

(6) (a) Duan, L.; Xu, Y.; Zhang, P.; Wang, M.; Sun, L. *Inorg. Chem.* **2010**, *49*, 209–215. (b) Kotani, H.; Suenobu, T.; Lee, Y.-M.; Nam, W.; Fukuzumi, S. *J. Am. Chem. Soc.* **2011**, *133*, 3249–3251. (c) Kalita, D.; Radaram, B.; Brooks, B.; Kannam, P. P.; Zhao, X. *ChemCatChem* **2011**, *3*, 571–573. (d) Li, F.; Yu, M.; Jiang, Y.; Huang, F.; Li, Y.; Zhang, B.; Sun, L. *Chem. Commun.* **2011**, *47*, 8949–8951. (e) Fukuzumi, S.; Mizuno, T.; Ojiri, T. *Chem.—Eur. J.* **2012**, *18*, 15794–15804. (f) Li, T. T.; Chen, Y.; Li, F. M.; Zhao, W. L.; Wang, C. J.; Lv, X. J.; Xu, Q. Q.; Fu, W. F. *Chem.—Eur. J.* **2014**, *20*, 8054–8061. (g) Ohzu, S.; Ishizuka, T.; Hirai, Y.; Fukuzumi, S.; Kojima, T. *Chem.—Eur. J.* **2013**, *19*, 1563–1567.

(7) (a) Carreno, M. C. *Chem. Rev.* **1995**, *95*, 1717–1760. (b) Fernandez, I.; Khair, N. *Chem. Rev.* **2003**, *103*, 3651–3706. (c) Ciclosi, M.; Dinioi, C.; Gonsalvi, L.; Peruzzini, M.; Manoury, E.; Poli, R. *Organometallics* **2008**, *27*, 2281–2286.

(8) (a) Barker, J. E.; Ren, T. *Tetrahedron Lett.* **2004**, *45*, 4681–4683. (b) Barker, J. E.; Ren, T. *Inorg. Chem.* **2008**, *47*, 2264–2266. (c) Bolm, C.; Bienewald, F. *Angew. Chem., Int. Ed.* **1996**, *34*, 2640–2642. (d) Kaczorowska, K.; Kolarska, Z.; Mitka, K.; Kowalski, P. *Tetrahedron* **2005**, *61*, 8315–8327. (e) Pitchen, P.; Dunach, E.; Deshmukh, M. N. *J. Am. Chem. Soc.* **1984**, *106*, 8188–8193.

(9) Hamelin, O.; Guillo, P.; Loiseau, F.; Boissonnet, M.-F.; Ménage, S. *Inorg. Chem.* **2011**, *50*, 7952–7954.

(10) (a) Huynh, M. H. V.; Dattelbaum, D. M.; Meyer, T. J. *Coord. Chem. Rev.* **2005**, *249*, 457–483. (b) Li, F.; Jiang, Y.; Zhang, B.; Huang, F.; Gao, Y.; Sun, L. *Angew. Chem., Int. Ed.* **2012**, *51*, 2417–2420. (c) Norris, M. R.; Concepcion, J. J.; Harrison, D. P.; Binstead, R. A.; Ashford, D. L.; Fang, Z.; Meyer, T. J. *J. Am. Chem. Soc.* **2013**, *135*, 2080–2083. (d) Kaveevivitchai, N.; Chitta, R.; Zong, R.; El Ojaimi, M.; Thummel, R. P. *J. Am. Chem. Soc.* **2012**, *134*, 10721–10724. (e) Farràs, P.; Maji, S.; Benet-Buchholz, J.; Llobet, A. *Chem.—Eur. J.* **2012**, *19*, 7162–7172.

(11) (a) Chao, D.; Fu, W. F. *Chem. Commun.* **2013**, *49*, 3872–3874. (b) Chao, D.; Fu, W. F. *Dalton Trans.* **2014**, *43*, 306–310. (c) Bian, Z. Y.; Chi, S. M.; Li, L.; Fu, W. *Dalton Trans.* **2010**, *39*, 7884–7887. (d) Schulz, M.; Karnahl, M.; Schwalbe, M.; Vos, J. G. *Coord. Chem. Rev.* **2012**, *256*, 1682–1705. (e) Gholamkhash, B.; Mametsuka, H.; Koike, K.; Tanabe, T.; Furue, M.; Ishitani, O. *Inorg. Chem.* **2005**, *44*, 2326–2336. (f) Bindra, G. *Dalton Trans.* **2011**, *40*, 10812–10814.

(12) Concepcion, J. J.; Jurss, J. W.; Templeton, J. L.; Meyer, T. J. *J. Am. Chem. Soc.* **2008**, *130*, 16462–16463.

(13) Chen, Z. F.; Chen, C. C.; Weinberg, D. R.; Kang, P.; Concepcion, J. J.; Harrison, D. P.; Brookhart, M. S.; Meyer, T. J. *Chem. Commun.* **2011**, *47*, 12607–12609.

- (14) (a) Broomhead, J. A.; Young, C. G. *Inorg. Synth.* **1982**, *21*, 127–128. (b) Takeuchi, K. J.; Thompson, M. S.; Pipes, D. W.; Meyer, T. J. *Inorg. Chem.* **1984**, *23*, 1845–1851.
- (15) (a) Sheldrick, G. M. *SHELXS 97, Program for the Solution of Crystal Structure*; University of Göttingen: Göttingen, Germany, 1997. (b) Sheldrick, G. M. *SHELXL97, Program for the Refinement of Crystal Structures*; University of Göttingen: Göttingen, Germany, 1997.
- (16) Guillo, P.; Hamelin, O.; Batat, P.; Jonusauskas, G.; McClenaghan, N. D.; Menage, S. *Inorg. Chem.* **2012**, *51*, 2222–2230.
- (17) (a) Yang, X.; Drepper, F.; Wu, B.; Sun, W.; Haehnel, W.; Janiak, C. *Dalton Trans.* **2005**, 256–267. (b) Gerli, A.; Reedijk, J.; Lakin, M. T.; Spek, A. L. *Inorg. Chem.* **1995**, *34*, 1836–1843.
- (18) McClanahan, S. F.; Dallinger, R. F.; Holler, F. J.; Kincaid, J. R. *J. Am. Chem. Soc.* **1985**, *107*, 4853–4860.
- (19) Herrero, C.; Quaranta, A.; Fallahpour, R. A.; Leibl, W.; Aukauloo, A. *J. Phys. Chem. C* **2013**, *117*, 9605–9612.
- (20) Swavey, S.; Fang, Z.; Brewer, K. J. *Inorg. Chem.* **2002**, *41*, 2598–2607.
- (21) (a) Chen, W.; Rein, F. N.; Rocha, R. C. *Angew. Chem., Int. Ed.* **2009**, *121*, 9852–9855. (b) Chen, W.; Rein, F. N.; Scott, B. L.; Rocha, R. C. *Chem.—Eur. J.* **2011**, *17*, 5595–5604.
- (22) (a) Sens, C.; Romero, I.; Rodríguez, M.; Llobet, A.; Parella, T.; Benet-Buchholz, J. *J. Am. Chem. Soc.* **2004**, *126*, 7798–7799. (b) Sala, X.; Romero, I.; Rodríguez, M.; Escriche, L.; Llobet, A. *Angew. Chem., Int. Ed.* **2009**, *48*, 2842–2852.
- (23) Masllorens, E.; Rodríguez, M.; Romero, I.; Roglans, A.; Parella, T.; Benet-Buchholz, J.; Poyatos, M.; Llobet, A. *J. Am. Chem. Soc.* **2006**, *128*, 5306–5307.
- (24) (a) Lehn, J.-M.; Sauvage, J.-P.; Ziessel, R. *Nouv. J. Chim.* **1979**, *3*, 423–427. (b) Harriman, A.; Porter, G.; Walters, P. *J. Chem. Soc., Faraday Trans.* **1981**, *77*, 2373–2383.
- (25) Concepcion, J. J.; Tsai, M.-K.; Muckerman, J. T.; Meyer, T. J. *J. Am. Chem. Soc.* **2010**, *132*, 1545–1557.